Effects of magnesium content on the physical, chemical and degradation properties in a MgO−CaO−Na 2 O−P 2 O 5 glass system

6 AUTHORS, INCLUDING:

In-Ho Lee
Dankook University
14 PUBLICATIONS **87** CITATIONS

SEE PROFILE

Farzad Foroutan
UCL Eastman Dental Institute
11 PUBLICATIONS **20** CITATIONS

SEE PROFILE

Nilay Lakhkar
SynThera Biomedical
14 PUBLICATIONS **123** CITATIONS

SEE PROFILE

Jonathan Campbell Knowles
University College London
396 PUBLICATIONS **9,515** CITATIONS

SEE PROFILE

Effects of magnesium content on the physical, chemical and degradation properties in a MgO—CaO—Na$_2$O—P$_2$O$_5$ glass system

In-Ho Lee [a], Song-Hee Shin [a], Farzad Foroutan [b], Nilay J. Lakhkar [b], Myoung-Seon Gong [a],*, Jonathan C. Knowles [a,b],**

[a] Department of Nanobiomedical Science and WCU Research Center of Nanobiomedical Science, Dankook University, Chungnam 330-714, Republic of Korea
[b] Division of Biomaterials and Tissue Engineering, Eastman Dental Institute, University College London, 256 Gray's Inn Road, London WC1X 8LD, UK

ARTICLE INFO

ABSTRACT

This paper presents the structural characterisation and degradation behavior of the glass system 20Na$_2$O–(30−X) CaO–XMgO–50P$_2$O$_5$ (X = 0, 5, 10, 15, 20, 25 and 30 mol%) wherein magnesium oxide is introduced as a partial calcium oxide substitute. This system is of interest from the viewpoint of investigating the subtle effects on structure and degradation that arise from the substitution of divalent ions (Mg^{2+} for Ca^{2+}) in these glass systems. Studies such as differential thermal analysis (DTA), Fourier transform infrared (FTIR) spectroscopy and ^{31}P nuclear magnetic resonance (NMR) reveal little change in the glass structure. However, degradation and ion release measurements for glass discs immersed in deionised water at 37 °C over a 21 day period highlight an inverse exponential effect between glass degradation rate and MgO content. Thus, the investigated glass systems provide interesting insights into the effects of parameters such as ionic radius, atomic weight and bond length on the glass properties. From an applications perspective, these glasses offer a selective range of degradation rates from highly degradable to relatively stable systems and can potentially serve as vehicles for the delivery of magnesium ions in the clinical realm.

1. Introduction

Biodegradable materials with their great potential in tissue engineering applications have been the subject of much interest in recent studies. Numerous bioactive glasses have been developed for repair and reconstruction of bone and tissue [1]. Ternary P$_2$O$_5$–CaO–Na$_2$O phosphate glasses have recently generated considerable interest as attractive materials for a variety of clinical applications such as dental implants, scaffolds for bone tissue engineering, and vehicles for antimicrobial ion delivery and drug release [2–4].

Phosphate based glasses are inorganic polymers composed of (PO$_4$)$^{3−}$ tetrahedra that are regarded as the backbone of the glass, and their chemistry can be manipulated during their manufacture [1,5–7]. However compositions such as Na$_2$O–CaO–P$_2$O$_5$ tend to have limited use primarily due to their very high dissolution rates which give rise to large pH changes. Several strategies have been employed to control the pH changes and these generally involve reducing the dissolution rate via addition of high valency ions [5,8,9], which can alter the degradation rate by several orders of magnitude; thus, dissolution rates can be reduced and materials with considerably long dissolution times can be synthesised. In particular, many studies have focused on metal oxide addition to the ternary phosphate glass system. These glasses can be engineered to provide a candidate substrate for synthetic orthopedic graft materials by inclusion of mineral elements such as Sr^{2+}, Na$^+$, Mg^{2+} and Zn^{2+} [10–13]. These elements are usually incorporated as oxides, which are considered as glass network modifiers, and they have been shown to alter the glass network structure and hence the glass properties [14–19]. These modifying oxides have been incorporated into ternary P$_2$O$_5$–CaO–Na$_2$O glass at the expense of CaO while maintaining both Na$_2$O and P$_2$O$_5$ constant, and this has yielded glass systems with relatively low degradation rates compared to the parent ternary compositions. Pure vitreous phosphorus pentoxide (P$_2$O$_5$) is chemically unstable on account of hydrolysis of the P—O—P bond by atmospheric moisture. The addition of metal oxides improves the phosphate glass stability because the P—O—M$^+$ (where M = metal cation) bond is generally more stable toward atmospheric hydrolysis or solution attack [20–22]. Among the various metal oxides investigated for this purpose, MgO is of interest from a biological viewpoint because Mg^{2+} is known to play a physiological role in positively influencing bone strength [19]. It is worth noting that in addition to glasses, Mg^{2+} can be substituted into apatites [23].

A relatively simple ternary Na$_2$O–CaO–P$_2$O$_5$ based glass system was synthesised and was described by Franks et al. [13]. In their study, it was possible to create soluble phosphate based glasses with a range of degradation rates from highly degradable to relatively stable glasses.

* Corresponding author. Tel.: +44 20 3456 1189; fax: +82 70 7154 2252.
** Correspondence to: J. C. Knowles, Department of Nanobiomedical Science and WCU Research Center of Nanobiomedical Science, Dankook University, Chungnam 330-714, Republic of Korea. Tel.: +44 20 3456 1189; fax: +82 70 7154 2252.
E-mail addresses: msgong@dankook.ac.kr (M.-S. Gong), j.knowles@ucl.ac.uk (J.C. Knowles).

However, the degradation rate of this system was relatively high and the associated pH changes were significantly large. Therefore, in the present study, MgO was introduced to partially replace CaO as a network modifier and evaluate the effect of incorporating magnesium oxide on the physicochemical and degradation properties of the manufactured glasses and to determine whether some further control over the degradation properties could be exerted by this substitution.

2. Materials and methods

2.1. Glass preparation

Sodium dihydrogen phosphate (NaH_2PO_4), calcium carbonate ($CaCO_3$), phosphorus pentoxide (P_2O_5), and magnesium oxide (MgO; BDH, Poole, UK) were used as precursors (all chemicals were above 98% purity), and a total of 7 compositions were prepared as listed in Table 1. The precursors were weighed out and placed into a Pt/10% Rh crucible (Type 71040, Johnson Matthey, Royston, UK). The precursors were heated in a furnace (Carbolite, RHF 1500, Sheffield, UK) at 700 °C for 1 h to allow for removal of H_2O and CO_2 and then melted at 1200 °C for 2 h. Upon removal of the crucible from the furnace, the melted glass was then poured into a pre-heated graphite mould at 350 °C for 1 h and the mould was then allowed to cool to room temperature in the furnace overnight to form glass rods of 12 mm diameter for each composition. The rods were then sectioned into approximately 2 mm thick discs using a Testbourne diamond saw with methanol used as a coolant.

2.2. X-ray diffraction analysis

XRD was carried out on glass powders to confirm the amorphous nature of the glasses. Measurements were carried out on a Bruker-D8 Advance Diffractometer (Brüker, UK) in flat plate geometry, using Ni filtered Cu $K\alpha$ radiation. Data were collected using a Lynx Eye detector at 2θ values from 10° to 100° with a step size of 0.02° and a count time of 12 s.

2.3. Density measurements

Density measurements were carried out in triplicate on glass discs using Archimedes' principle. An analytical balance (± 0.1 mg, Mettler Toledo, UK) with an attached density kit was used for this purpose. Ethanol was used as the immersion liquid since the glasses are water soluble in nature.

2.4. Differential thermal analysis

The DTA experiments were carried out using a Setaram Differential Thermal Analyzer (Setaram, France) to measure the glass transition temperature (T_g). For this purpose, glass powder samples were heated from room temperature to 1000 °C at a heating rate of 20 °C min^{-1} using air as the purge gas. The DTA experiment was performed in duplicate for all the samples.

Table 1
Glass compositions and codes used.

Glass code	Glass composition (mol%)			
	P_2O_5	Na_2O	CaO	MgO
Mg0	50	20	30	0
Mg5	50	20	25	5
Mg10	50	20	20	10
Mg15	50	20	15	15
Mg20	50	20	10	20
Mg25	50	20	5	25
Mg30	50	20	0	30

2.5. Surface free energy

Glass discs from each composition were abraded and polished using waterproof silicon carbide papers (P #1200, Struers). The test liquids i.e. ultrapure water and n-hexadecane were used to represent both polar and non-polar characteristics respectively. The static contact angle was measured using a KSV Cam200 contact angle system (L. O. T-Oriel, UK). Droplets of ~5 μL of the test liquid were placed on the glass surface using a manual syringe. The drop profile was recorded at 0.04 s intervals for 2 s, and the measurements were carried out on triplicate samples. The surface free energy (SFE) was calculated on the basis of the obtained contact angle data using the Owens–Wendt–Rabel–Kaelble (OWRK) method, for which contact angle measurements of two or more drops including both polar and non-polar liquids were used [24,25].

2.6. Fourier transform infrared spectroscopy

FTIR spectra of the glasses were collected using a Bio-Rad Excaliber TS-3000MX spectrometer (Bio-Rad, Tokyo, Japan). Glass powders were scanned in the transmittance mode in the range 4000–400 cm^{-1}. Each spectrum was the result of averaging 10 scans.

2.7. Solid state nuclear magnetic resonance

Solid-state ^{31}P MAS NMR spectra were recorded at 161.87 MHz using a Varian VNMRS400 spectrometer for which glass powders were loaded into a 4 mm (rotor o.d.) magic-angle spinning probe. The spectra were obtained using direct excitation (with a 90° pulse) with a 60s recycle delay at ambient probe temperature (~25 °C) and at a sample spin rate of 10 kHz. Between 20 and 88 repetitions were accumulated. Spectral referencing was with respect to an external sample of 85% H_3PO_4. Deconvolution of the ^{31}P MAS NMR spectra was carried out using DMFit software [26].

2.8. Degradation study

The degradation studies were carried out on triplicate glass disc specimens in deionised water at 37 ± 1 °C using a weight loss method. The surface area of the glass discs was calculated from dimensions obtained via a pair of Mitutoyo Digimatic vernier calipers. Glass discs were placed in containers holding 25 ml of high purity water obtained from a PURELAB UHQ-PS (Elga Labwater, UK; resistivity = 18.2 MΩ cm^{-1}). The water pH had been adjusted to 7 ± 0.1 using NH_4OH and HCl prior to use. At various time points up to 500 h, the samples were removed from the solution, which was stored for pH and ion release measurements (see below), dried with tissue and weighed, and then placed in a fresh solution of pH-adjusted deionised water and replaced in the incubator at 37 ± 1 °C. The following equation was used to calculate the percent weight loss per unit surface area:

$$(M_0 - M_t)/(M_0 \times A) \times 100$$

where M_0 is the original weight of the glass disc (mg); M_t, the weight of the glass disc at time t (mg); and A, the surface area of the glass disc (cm^2). The degradation rate was measured in terms of the slope of the trend line in the graph of percentage weight loss per unit surface area versus time plotted for each composition.

2.9. pH change

The pH of the post-degradation medium was measured using an Orion pH meter (Orion, UK) with a pH glass electrode (BDH, UK). The meter was calibrated using colourkey standard solutions (BDH, UK) every time before use.

2.10. Ion release analysis

The degradation medium was analysed simultaneously for cation (Na^+, Ca^{2+} and Mg^{2+}) and anion (PO_4^{3-}, $P_2O_7^{4-}$, $P_3O_9^{3-}$, and $P_3O_{10}^{5-}$) release using ion chromatography techniques (Dionex, UK) in accordance with previously described methods [9]. For anion chromatography, no further purification of the liquid was required, but for cation chromatography, the liquid was passed through a Dionex Onguard IIA cartridge to remove anions that might bind to the cation column. The ion release rate was measured in terms of the slope of the trend line in the graph of ion release versus time plotted for each composition.

3. Results

3.1. X-ray diffraction analysis

The XRD patterns for different glass samples (data not shown) were free from any detectable crystalline phases and broad peaks were observed at 2θ values around 20–40°. This finding confirmed the glassy amorphous nature of all the samples.

3.2. Density measurements

The density measurements (Fig. 1) revealed a decrease in density with an increase in the MgO content of the glass. Thus the glass density reduced from around 2.596 g cm^{-3} for Mg0 to around 2.555 g cm^{-3} for Mg30.

3.3. Differential thermal analysis

In contrast to the density results, the DTA results (Fig. 2) clearly showed an increase in the T_g value with the MgO content. Thus, the T_g value for the investigated glasses increased from 397.4 °C for Mg0 up to 437.5 °C for Mg30.

3.4. Surface free energy

All the investigated glasses exhibited contact angles in the range of 40–60° (Table 2). In the case of individual compositions, the contact angle in water was generally greater than that in n-hexadecane, although the difference in most cases was not considered significant since it was within the range of the standard deviation. The total SFE values of all glasses were in the range 50–60 mNm^{-1}. For individual glasses, the polar component of the SFE values was greater than the dispersive component. Neither the contact angle values nor
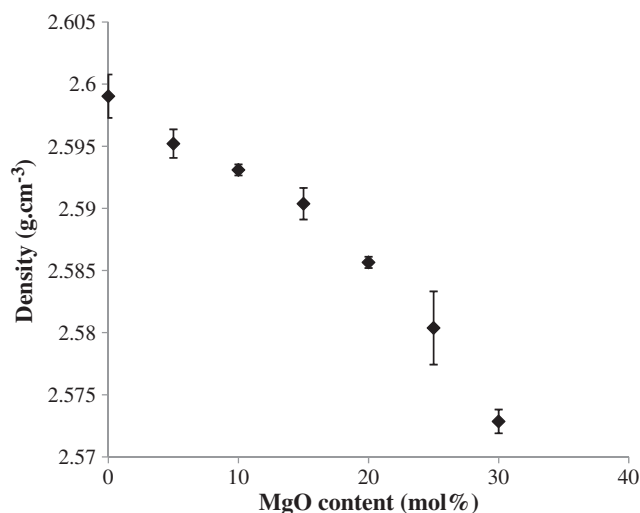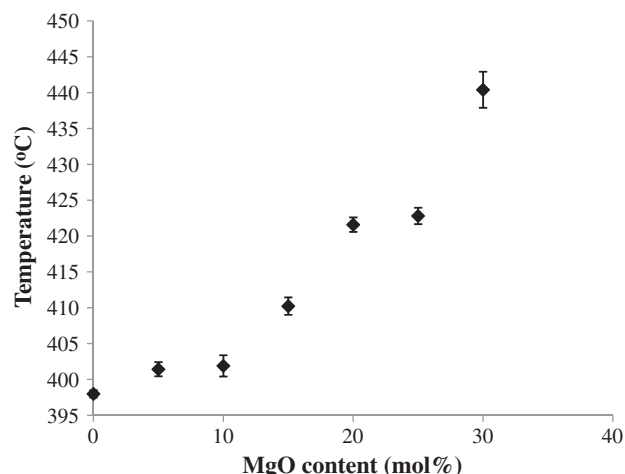
Fig. 2. Glass transition temperature (T_g) for magnesium phosphate glasses with different MgO contents.

the SFE values revealed any discernible trend with regard to the MgO content of the glasses.

3.5. Fourier transform infrared spectroscopy

The FTIR spectra of these glasses are presented in Fig. 3. The absorption bands were assigned according to previous FTIR studies on phosphate based glasses [27–30]. The band at 1250–1300 cm^{-1} was assigned to asymmetric stretching modes, v_{as} (PO^2), of the two non-bridging oxygen atoms bonded to a phosphorus atom in a Q^2 phosphate tetrahedron. The absorption bands v_{as}(P—O—P) and v_s(P—O—P) occurring at ~900 and 750 cm^{-1} were assigned, respectively, to the asymmetric and symmetric stretching of the bridging oxygen atoms bonded to a phosphorus atom in a Q^2 phosphate tetrahedron. The main change observed was a reduction in the intensity and a slight shift towards higher wavenumber values of the v_{as} (P—O—P) band (at approx. 900 cm^{-1}) and v_{as} (O—P—O) band (at 1253 cm^{-1}) as the Mg^{2+} content was increased.

3.6. Solid state nuclear magnetic resonance

In the NMR spectra of the studied magnesium phosphate glasses (Fig. 4a), virtually all the glasses showed a peak at around −25 ppm. A small peak at around −16 ppm (and estimated to be less than 2% of the total) was observed for Mg0, Mg5 and Mg10, i.e. samples with low glass content, but this peak disappeared at higher MgO contents. Following deconvolution of the data, two further parameters—the line width and chemical shift could be measured and they were plotted against the MgO content (Fig. 4b). With an increase in the MgO content, the line width showed a slow and relatively linear decrease while the chemical shift showed a gradual change to less negative values.

3.7. Degradation study

Fig. 5 shows the percentage cumulative weight loss per unit surface area as a function of the degradation time for glass discs of all the investigated magnesium phosphate glass compositions. Table 3 lists the degradation rate in terms of the slope of the trend line plotted for each composition (trend lines not shown in the graph). Note that the degradation rates obtained from the linear fits were used only as a means to rank the degradation behavior of the glass compositions and should not be considered as representative of linear degradation behavior. It was clearly observed that all glasses showed increased degradation with time. Furthermore, the degradation rate decreased significantly with an increase in the MgO content. Thus,

Fig. 1. Density of the investigated glass compositions as a function of the MgO content.

Table 2
Total surface free energy (SFE^{tot} in mN/m) with the dispersive (SFE^d) and polar components (SFE^p) of phosphate glasses with different calcium and magnesium contents according to the OWRK method, and contact angle measurements (°) with ultrapure water (CA^{H2O}) and n-hexadecane (CA^{C16H34}) as test liquids.

Sample	SFE^d	St Dev	SFE^p	St Dev	SFE^{tot}	St Dev	CA^{H2O} (°)	St Dev	CA^{C16H34} (°)	St Dev
Mg0	23.255	0.841	34.600	2.687	57.855	3.528	40.826	3.218	31.998	3.401
Mg5	23.443	0.305	32.373	5.206	55.816	4.901	48.305	3.706	33.544	1.427
Mg10	22.630	0.396	37.926	3.584	60.556	3.970	35.865	6.895	35.863	1.375
Mg15	23.183	0.907	33.030	3.876	56.206	3.732	42.969	5.338	33.192	3.607
Mg20	22.600	0.269	36.400	2.450	59.000	2.593	38.282	4.409	35.968	1.443
Mg25	23.503	0.863	32.750	2.265	56.256	2.641	42.782	3.876	32.216	3.785
Mg30	22.810	0.935	31.443	8.564	54.253	7.631	39.646	8.118	35.059	3.665

while Mg0 showed the highest degradation rate among all the investigated glasses at 5.97×10^{-2} %cm^{-2} h^{-1}, the addition of 5 mol% MgO led to an approximate 50% reduction in the degradation rate to 2.55×10^{-2} %cm^{-2} h^{-1}. Further incorporation of MgO in the glass led to similar levels of reduction (approx. 50%) in the degradation rate in successive glass compositions up to Mg20; at higher MgO contents (i.e. in Mg25 and Mg30), the decrease in the degradation rate was less pronounced.

3.8. pH change

For all the investigated magnesium phosphate glasses, the pH reduced at 24 h but then increased at 72 h (Fig. 6). After 72 h, all the glasses showed a net decrease in pH over the rest of the study period, although glasses with lower MgO contents (Mg0, Mg5, Mg10 and Mg15) showed a sharper decrease (particularly apparent between 168 and 336 h) than the remaining glasses.

3.9. Ion release analysis

Figs. 7 and 8 show the cumulative release of Ca^{2+} cations and PO$_4^{3-}$ anions as a function of time for the studied glass compositions; similar to the degradation graph (Fig. 5), the ion release rate was obtained by measuring the slope of the trend line for each composition (the release of Na$^+$ and Mg^{2+} cations as well as P$_3$O$_9^{3-}$, P$_2$O$_7^{4-}$ and P$_3$O$_{10}^{5-}$ anions follows the same trend and the ion release data for these ions have been tabulated in Table 3). Note that as in the case of the degradation plot, the ion release rates obtained from the linear fits were used only as a means to rank the ion release behavior of the glass compositions and should not be considered as representative of linear ion release behavior. Similar to the degradation results, the ion release increased with time for all the investigated ions and the release rates of all ions decreased with an increase in the MgO content, with the extent of decrease being greater at lower MgO contents (up to Mg20).
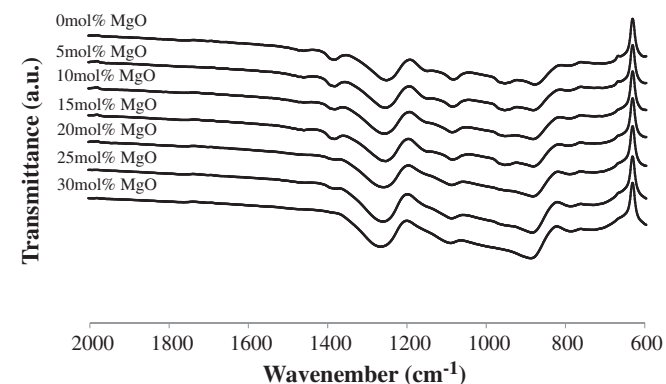
4. Discussion

The glass systems investigated in the present study are of interest from the viewpoints of both the glass structure as well as potential applications. The progressive replacement of Ca^{2+} ions in P$_2$O$_5$–Na$_2$O–CaO with Mg^{2+} ions provides the opportunity to investigate the more subtle effects brought about by metal ion incorporation in cases where ionic charge is effectively eliminated as an influencing factor, and several interesting results have been obtained in this regard.

For the purposes of this study, XRD serves as a basic tool to test the success of the glass production process; the absence of crystalline peaks directly indicates the amorphous glassy nature of all the investigated compositions. The increase in T_g on one hand and decrease in glass density on the other as the MgO content of the glasses is increased might seem to be contrasting results. To elaborate, in the case of glass systems such as P$_2$O$_5$–Na$_2$O–CaO–Fe$_2$O$_3$ and P$_2$O$_5$–Na$_2$O–CaO–TiO$_2$, both the glass density and T_g tend to increase as the metal oxide content is increased at the expense of either Na$_2$O or CaO [31–34]; the main reason for those findings is the incorporation of a metallic ion of higher charge
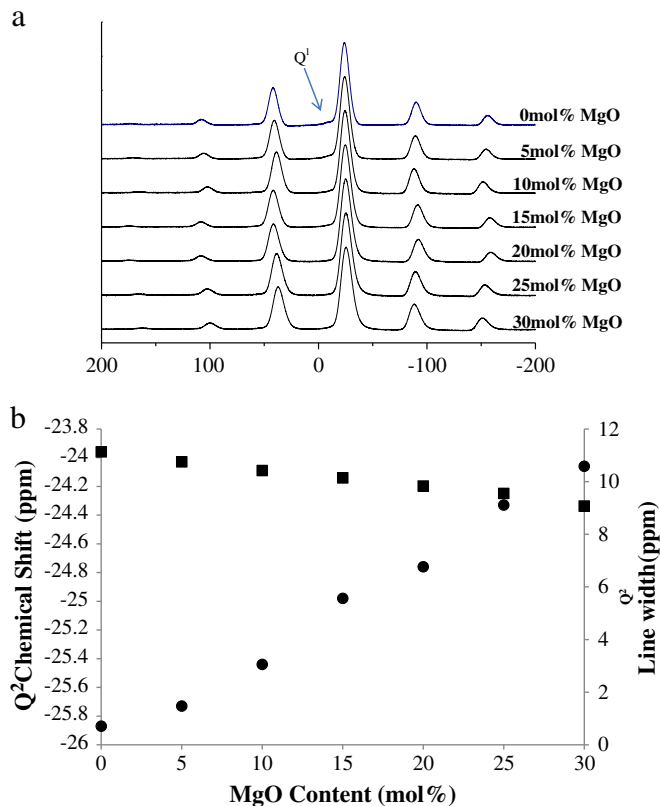

Fig. 3. Fourier transform infrared (FTIR) spectra of the investigated glass compositions.

Fig. 4a. ^{31}P nuclear magnetic resonance (NMR) spectra of magnesium phosphate glasses with different MgO contents. b. Q^2 ^{31}P Chemical shifts (●) and line widths (■) against MgO content.
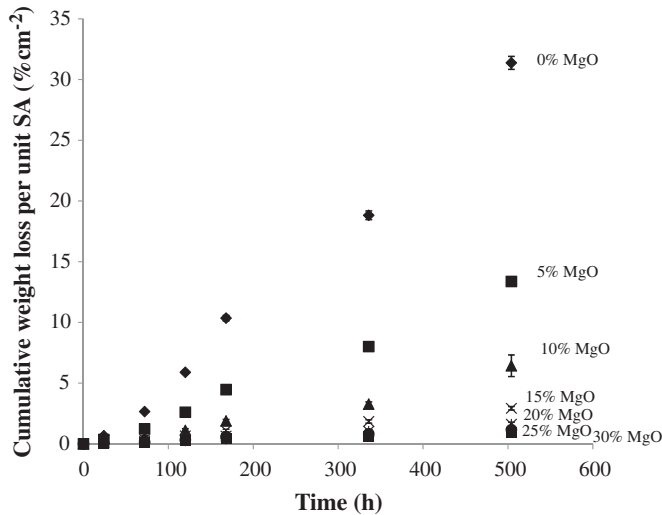
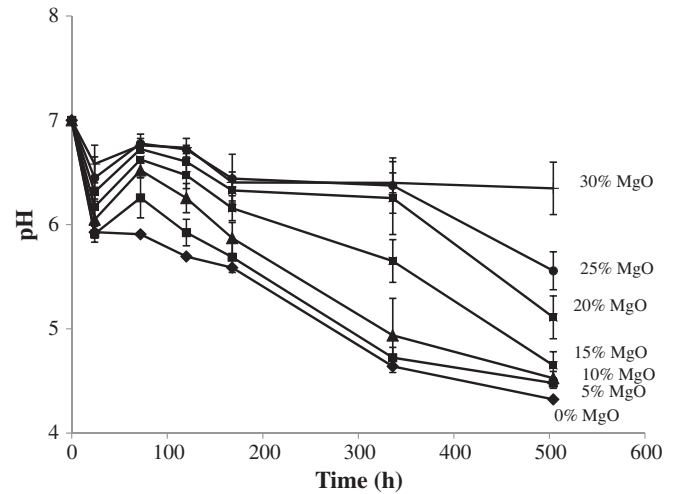Fig. 5. Degradation in terms of percentage cumulative weight loss per unit surface area ($\%cm^{-2}$) as a function of time for the studied glass systems.

Fig. 6. pH changes in deionised water at 37 °C as a function of time for the investigated magnesium phosphate glasses.

(Fe^{3+} or Ti^{4+}) in the glass network which serves to increase the atomic packing and strengthen the glass structure.

In the present study, however, the difference in the T_g and density findings can be explained in a different way. In the case of glass density, the atomic weight of the ions is considered to play an important role. The relative atomic weight of calcium (40.078) is close to two times that of magnesium (24.305) [35]. Thus, since the glass density is a function of the sample mass, replacement of a heavier ion with a lighter one would lead to a decrease in density. On the other hand, the T_g value is related to the bond strength of the glass network, which can be expressed in terms of the bond length; the smaller the bond length, the stronger the bond formed between the constituent atoms [36,37]. The bond strength is affected by the cation field strength (which is the charge divided by the square of the cation–oxygen distance), and for the alkaline earth cations in the glasses in this study, these are 0.46 for Mg^{2+} and 0.36 for Ca^{2+}. Because of the higher field strength, the bond length of Mg–O (0.204 nm) is smaller than that of Ca–O (0.233 nm). Therefore, Mg^{2+} bonds are stronger than Ca^{2+} bonds and more energy would be required to break these bonds [36,38,39], thereby resulting in a higher T_g value. The difference in ionic radius between Mg^{2+} (86 pm) and Ca^{2+} (114 pm) is also considered to play a role. These results parallel those found when swapping Ca^{2+} for Zn^{2+} in zinc phosphate glasses [25,40], although it should be noted that in the case of the zinc glasses, a decrease in T_g and increase in glass density is observed with increased ZnO incorporation.

Only minor changes, if at all, can be discerned in the contact angle, surface free energy, FTIR and ^{31}P NMR results. The lack of significant difference in the contact angle results indicates that the glass surface is neither strongly hydrophilic nor strongly hydrophobic in nature.

The relatively larger value of the polar SFE component in comparison with the dispersive component seems to indicate a slight dominance of the polar characteristics of the investigated glasses, which can be attributed to the P—O—P bonds present in the glass structure. The absence of any influence of the MgO content on the contact angle and SFE values can be expected since the level of MgO incorporation is not sufficiently high to influence the surface wettability characteristics of the glass. With regard to the FTIR results, the reduction in the intensity and a slight shift towards higher wavenumber values of the v_{as} (P—O—P) band (at approx. 900 cm^{-1}) and v_{as} (O—P—O) band (at 1253 cm^{-1}) as the Mg^{2+} content is increased can be explained by the field strength of the cation and an increase in the O—P—O or P—O—P bond angles for the alkaline-earth cation in the glasses [41,42]. The v_{as} (P—O—P) bond angle decreases with increasing cation field strength. Since the field strength of Ca^{2+} is lower than that of Mg^{2+}, the P—O—P bond angle decreases with substitution of MgO for CaO, causing the v_{as} (P—O—P) absorption bands to shift towards higher wavenumber values. However, from an overall perspective, the spectra from the magnesium-containing glasses can be considered to show only very subtle variation as a function of composition.

The NMR spectra of the studied magnesium phosphate glasses show some evidence for very small levels of Q^1 in the melt, and the presence of a peak at around −25 ppm in almost all the glasses indicates the
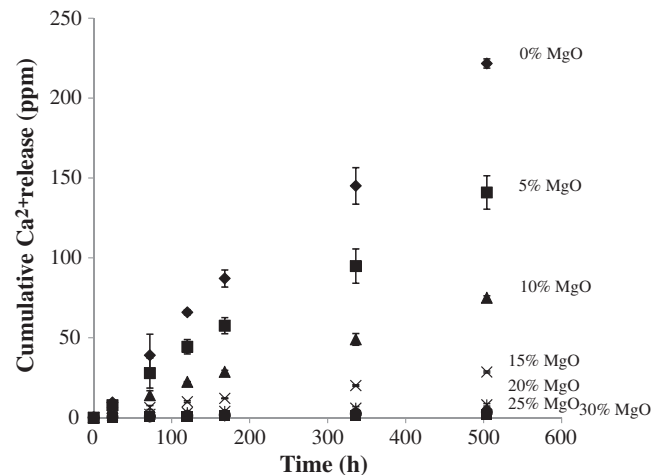
Table 3
Cumulative cation and anion release rate (ppm h^{-1} 10^{-2}) calculated from the slope of the linear fit of ion release against time for the investigated glass compositions.

Glass code	Degradation rate ($\%cm^{-2}$ h^{-1} 10^{-2})	Cation (ppm h^{-1} 10^{-2})			Anion (ppm h^{-1} 10^{-2})			
		Na^+	Ca^{2+}	Mg^{2+}	PO_4^{3-}	$P_3O_9^{3-}$	$P_2O_7^{4-}$	$P_3O_{10}^{5-}$
Mg0	5.97	65.41	44.81	–	53.8	520	4.01	40.4
Mg5	2.55	38.99	28.92	5.81	17.48	166	2.52	13.27
Mg10	1.16	21.5	15.15	5.14	5.69	40.46	1.65	6.37
Mg15	0.57	11.1	6	4.61	2.59	21.24	0.7	3.58
Mg20	0.32	5.49	1.74	3.9	1	7.98	0.4	1.53
Mg25	0.24	3.45	0.74	2.79	0.83	2.94	0.07	0.71
Mg30	0.19	3.12	0.44	2.33	0.69	2.25	0.05	0.51

Fig. 7. Cumulative release of Ca^{2+} cations (ppm) as a function of time for the investigated glasses.
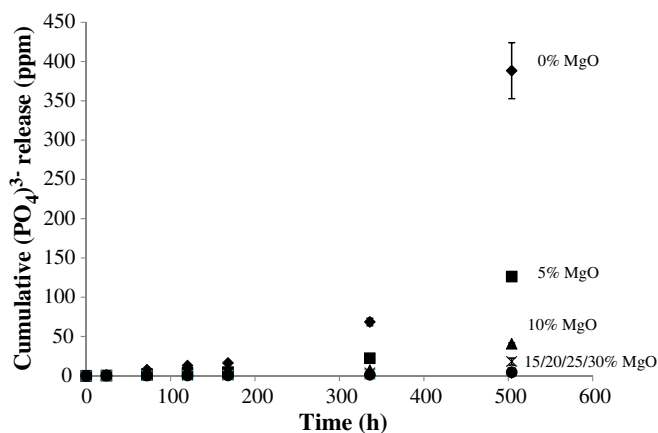
Fig. 8. Cumulative release of PO_4^{3-} anions (ppm) as a function of time for the investigated glasses.

presence of Q^2 species. In fact, apart from a relatively small change in Q species at low MgO content, little structural change as measured by ^{31}P NMR can be discerned and we would expect these glasses to consist of predominantly Q^2 units [8]. The small peak observed at around -16 ppm in the Mg0, Mg5 and Mg10 spectra is consistent with the presence of Q^1 species and is estimated to be at around 2% or less of the total Q speciation; however, this peak disappears at higher MgO contents. Analysis of the Q^2 line widths and chemical shifts revealed a decrease in line width with increasing MgO content, indicating a move to a more ordered structure [43] and perhaps a decrease in the range of phosphate tetrahedral bond lengths [44]. This also correlates with the findings of Brow et al. [45]. ^{31}P NMR chemical shift is sensitive to the electronegativity, the radius and the charge of the next-nearest-neighbor cations, and indicates that ^{31}P chemical shifts may reveal some of the details of cation environments in complex, amorphous systems, such as certain glass systems [46]. Data for the chemical shift showed a change to less negative values with increasing MgO content; this can be related to a decrease in shielding, and this decrease in shielding (more positive chemical shift) with decreasing polymerisation (fewer bridging oxygens per tetrahedron) may be due to the increased ionicity of the non-bridging oxygen bonds [47]. The glass composition can also affect the chemical shifts. Each peak becomes less shielded with increasing CaO content. Similar changes in chemical shifts have been noted in other NMR studies of phosphate glasses [44] and indicate electron density redistribution among tetrahedra with changing bridging to non-bridging oxygen ratios.

As in the case of glass density and T_g, the trends observed in the degradation, pH and ion release rates seem to be determined by differences in the relative atomic weights and atomic radii of the Ca and Mg atoms and in the bond lengths of the Ca—O and Mg—O bonds. The successive addition of 5 mol% MgO up to about 25 mol% is generally sufficient to reduce both the degradation and the individual ion release rates from one composition to the next by a minimum of almost 80–100% (with the exception of the Mg^{2+} ions). Thus, it is clear that up to about 25 mol% MgO, the incorporation of Mg^{2+} ions in the glass structure at the expense of Ca^{2+} ions serves to significantly densify the glass structure. Beyond 25 mol%, further MgO addition does not affect the degradation and ion release rates to the same extent, suggesting the onset of a saturation effect, which has been widely observed in different glass systems [1,5]. The ion release rates for cations appear to be linear, whereas those for the polyphosphate anions appear to be exponential. However, it is not possible for us to unequivocally confirm that the release rates follow a linear or exponential trend. As such, the use of linear trend lines to obtain the degradation and ion release rates is purely a means to rank the degradation and ion release behavior of the different compositions. The values of the ion release rates show that among cations and anions, the Na^+ and $P_3O_9^{3-}$ ions have the maximum release

rates respectively. This result has been observed in several previous studies and seems to suggest that these ions are present in the original glass structure to the greatest extent [31]. With regard to the observed pH changes, the initial reduction in pH for all the investigated glasses at 24 h seems to be related to the hydrated phosphate chains dissociating into the solution. However, the pH value increases from 24 to 72 h, which may be related to the presence of Na^+ ions in the solution. The subsequent downward trend in pH is attributable to the increasing release of polyphosphates which tend to bond with protons to form phosphoric acid. At a high MgO content of 30 mol%, the pH remains relatively stable over time, which correlates well with the ion release and degradation results.

Thus, from the structural viewpoint, the results of studies on the investigated glass compositions clearly indicate that even when the ionic charge of the dopant is not a influencing factor, there are other factors such as ionic radius, atomic weight and bond lengths that may be responsible for the significant changes in glass degradation behaviour and ion release. From the viewpoint of applications, these glasses could serve as vehicles for *in vivo* Mg^{2+} ion delivery, although further studies need to be carried out in order to optimise the glass composition for effective Mg^{2+} release in clinical environments. Many previous studies have confirmed the role played by magnesium in various physiological processes including bone formation, parathyroid gland function and vitamin D metabolism [12,23,48–50]. In this context, the results of the present study demonstrate that the investigated glass compositions merit further attention.

5. Conclusion

Melt-derived magnesium phosphate glasses having compositions $20Na_2O–(30−X)CaO–XMgO–50P_2O_5$ ($X = 0$, 5, 10, 15, 20, 25 and 30 mol%) were synthesised and investigated with a view to probing the effects on glass structure and properties when substituting Mg^{2+} ions in place of Ca^{2+} ions. The variation in MgO content led to contrasting trends in glass density on one hand and T_g on the other, but it did not cause considerable changes in the glass surface and bulk structure as revealed by surface free energy, FTIR and ^{31}P NMR studies, although some subtle variations in ^{31}P NMR line widths and chemical shifts were observed. The degradation and ion release studies revealed the decreasing degradation rate of the glass systems with an increase in MgO content. Taken together, the results demonstrated the subtle effects of factors such as ionic radius, cation field strength, atomic weight and bond lengths on the structure and properties of glasses when ionic charge does not constitute an influencing factor. From an applications perspective, the glasses could potentially serve as *in vivo* magnesium ion delivery systems, although further studies will be required to optimise the glass composition for this purpose.

References

[1] I. Ahmed, C.A. Collins, M.P. Lewis, I. Olsen, J.C. Knowles, Processing, characterisation and biocompatibility of iron-phosphate glass fibres for tissue engineering, Biomaterials 25 (2004) 3223–3232.
[2] J.C. Knowles, Phosphate based glasses for biomedical applications, J. Mater. Chem. 13 (2003) 2395–2401.
[3] I. Ahmed, D. Ready, M. Wilson, J.C. Knowles, Antimicrobial effect of silver-doped phosphate-based glasses, J Biomed Mater Res A 79A (2006) 618–626.
[4] C.F. Drake, W.M. Allen, The use of controlled-release glass for the controlled delivery of bioactive materials, Biochem. Soc. Trans. 13 (1985) 516–520.
[5] E.A. Abou Neel, I. Ahmed, J.J. Blaker, A. Bismarck, A.R. Boccaccini, M.P. Lewis, S.N. Nazhat, J.C. Knowles, Effect of iron on the surface, degradation and ion release properties of phosphate-based glass fibres, Acta Biomater. 1 (2005) 553–563.

[6] E.A. Abou Neel, I. Ahmed, J. Pratten, S.N. Nazhat, J.C. Knowles, Characterisation of antibacterial copper releasing degradable phosphate glass fibres, Biomaterials 26 (2005) 2247–2254.

[7] K.L. Skelton, J.V. Glenn, S.A. Clarke, G. Georgiou, S.P. Valappil, C. Knowles, S.N. Nazhat, G.R. Jordan, Effect of ternary phosphate-based glass compositions on osteoblast and osteoblast-like proliferation, differentiation and death in vitro, Acta Biomater. 3 (2007) 563–572.

[8] E.A. Abou Neel, W. Chrzanowski, S.P. Valappil, L.A. O'Dell, D.M. Pickup, M.E. Smith, R.J. Newport, J.C. Knowles, Doping of a high calcium oxide metaphosphate glass with titanium dioxide, J. Non-Cryst. Solids 355 (2009) 991–1000.

[9] E.A. Abou Neel, J.C. Knowles, Physical and biocompatibility studies of novel titanium dioxide doped phosphate-based glasses for bone tissue engineering applications, J. Mater. Sci. Mater. Med. 19 (2008) 377–386.

[10] A. Ito, K. Ojima, H. Naito, N. Ichinose, T. Tateishi, Preparation, solubility, and cytocompatibility of zinc-releasing calcium phosphate ceramics, J. Biomed. Mater. Res. 50 (2000) 178–183.

[11] P. Ammann, I. Badoud, S. Barraud, R. Dayer, R. Rizzoli, Strontium ranelate treatment improves trabecular and cortical intrinsic bone tissue quality, a determinant of bone strength, J. Bone Miner. Res. 22 (2007) 1419–1425.

[12] T. Okuma, Magnesium and bone strength, Nutrition 17 (2001) 679–680.

[13] K. Franks, I. Abrahams, J.C. Knowles, Development of soluble glasses for biomedical use Part I: in vitro solubility measurement, J. Mater. Sci. Mater. Med. 11 (2000) 609–614.

[14] K. Franks, V. Salih, J.C. Knowles, I. Olsen, The effect of MgO on the solubility behavior and cell proliferation in a quaternary soluble phosphate based glass system, J. Mater. Sci. Mater. Med. 13 (2002) 549–556.

[15] K. Franks, I. Abrahams, G. Georgiou, J.C. Knowles, Investigation of thermal parameters and crystallisation in a ternary CaO–Na(2)O–P(2)O(5)-based glass system, Biomaterials 22 (2001) 497–501.

[16] V. Salih, A. Patel, J.C. Knowles, Zinc-containing phosphate-based glasses for tissue engineering, Biomed. Mater. 2 (2007) 11–20.

[17] J.E. Gough, P. Christian, C.A. Scotchford, I.A. Jones, Long-term craniofacial osteoblast culture on a sodium phosphate and a calcium/sodium phosphate glass, J. Biomed. Mater. Res. A 66A (2003) 233–240.

[18] M. Bitar, V. Salih, V. Mudera, J.C. Knowles, M.P. Lewis, Soluble phosphate glasses: in vitro studies using human cells of hard and soft tissue origin, Biomaterials 25 (2004) 2283–2292.

[19] V. Salih, K. Franks, M. James, G.W. Hastings, J.C. Knowles, I. Olsen, Development of soluble glasses for biomedical use Part II: the biological response of human osteoblast cell lines to phosphate-based soluble glasses, J. Mater. Sci. Mater. Med. 11 (2000) 615–620.

[20] B.S. Bae, M.C. Weinberg, Oxidation-reduction equilibrium in copper phosphate-glass melted in air, J. Am. Ceram. Soc. 74 (1991) 3039–3045.

[21] K.V. Shah, M. Goswami, S. Manikandan, V.K. Shrikhande, G.P. Kothiyal, Surface degradation behaviour of sodium borophosphate glass in aqueous media: some studies, Bull. Mater. Sci. 32 (2009) 329–336.

[22] A.S. Monem, H.A. ElBatal, E.M.A. Khalil, M.A. Azooz, Y.M. Hamdy, In vivo behavior of bioactive phosphate glass-ceramics from the system P(2)O(5)–Na(2)O–CaO containing TiO(2), J. Mater. Sci. Mater. Med. 19 (2008) 1097–1108.

[23] D. Laurencin, N. Almora-Barrios, N.H. de Leeuw, C. Gervais, C. Bonhomme, F. Mauri, W. Chrzanowski, J.C. Knowles, R.J. Newport, A. Wong, Z. Gan, M.E. Smith, Magnesium incorporation into hydroxyapatite, Biomaterials 32 (2011) 1826–1837.

[24] E.A. Abou Neel, L.A. O'Dell, W. Chrzanowski, M.E. Smith, J.C. Knowles, Control of surface free energy in titanium doped phosphate based glasses by co-doping with zinc, J. Biomed. Mater. Res. 89B (2009) 392–407.

[25] E.A. Abou Neel, L.A. O'Dell, M.E. Smith, J.C. Knowles, Processing, characterisation, and biocompatibility of zinc modified metaphosphate based glasses for biomedical applications, J. Mater. Sci. Mater. Med. 19 (2008) 1669–1679.

[26] D. Massiot, F. Fayon, M. Capron, I. King, S. Le Calve, B. Alonso, J.O. Durand, B. Bujoli, Z.H. Gan, G. Hoatson, Modelling one- and two-dimensional solid-state NMR spectra, Magn. Reson. Chem. 40 (2002) 70–76.

[27] J.-O. Byun, B.-H. Kim, K.-S. Hong, H.-J. Jung, S.-W. Lee, A.A. Izyneev, Properties and structure of RO–Na2O–Al2O3–P2O5 (R = Mg, Ca, Sr, Ba) glasses, J. Non-Cryst. Solids 190 (1995) 288–295.

[28] Y.M. Moustafa, K. El-Egili, Infrared spectra of sodium phosphate glasses, J. Non-Cryst. Solids 240 (1998) 144–153.

[29] L. Baia, D. Muresan, M. Baia, J. Popp, S. Simon, Structural properties of silver nanoclusters-phosphate glass composites, Vib. Spectrosc. 43 (2007) 313–318.

[30] D. Ilieva, B. Jivov, G. Bogachev, C. Petkov, I. Penkov, Y. Dimitriev, Infrared and raman spectra of Ga2O3–O5 glasses, J. Non-Cryst. Solids 283 (2001) 195–202.

[31] E.A. Abou Neel, T. Mizoguchi, M. Ito, M. Bitar, V. Salih, J.C. Knowles, In vitro bioactivity and gene expression by cells cultured on titanium dioxide doped phosphate-based glasses, Biomaterials 28 (2007) 2967–2977.

[32] E.A. Abou Neel, W. Chrzanowski, J.C. Knowles, Effect of increasing titanium dioxide content on bulk and surface properties of phosphate-based glasses, Acta Biomater. 4 (2008) 523–534.

[33] H.A. ElBatal, E.M.A. Khalil, Y.M. Hamdy, In vitro behavior of bioactive phosphate glass-ceramics from the system P2O5–Na2O–CaO containing titania, Ceram. Int. 35 (2009) 1195–1204.

[34] R.C. Lucacel, M. Maier, V. Simon, Structural and in vitro characterization of TiO2–CaO–P2O5 bioglasses, J. Non-Cryst. Solids 356 (2010) 2869–2874.

[35] M.E. Wieser, T.B. Coplen, Atomic weights of the elements 2009 (IUPAC Technical Report), Pure Appl. Chem. 83 (2011) 359–396.

[36] U. Hoppe, A structural model for phosphate glasses, J. Non-Cryst. Solids 195 (1996) 138–147.

[37] L.L. Velli, C.P.E. Varsamis, E.I. Kamitsos, D. Moncke, D. Ehrt, Structural investigation of metaphosphate glasses, Phys. Chem. Glasses 46 (2005) 178–181.

[38] G. Walter, J. Vogel, U. Hoppe, P. Hartmann, The structure of CaO–Na2O–MgO–P2O5 invert glass, J. Non-Cryst. Solids 296 (2001) 212–223.

[39] K.M. Wetherall, D.M. Pickup, R.J. Newport, G. Mountjoy, The structure of calcium metaphosphate glass obtained from x-ray and neutron diffraction and reverse Monte Carlo modelling, J. Phys. Condens. Matter 21 (2009).

[40] V. Salih, A. Patel, J.C. Knowles, Zinc-containing phosphate-based glasses for tissue engineering, Biomed. Mater. 2 (2007) 11–20.

[41] K. Meyer, Characterization of the structure of binary zinc ultraphosphate glasses by infrared and Raman spectroscopy, J. Non-Cryst. Solids 209 (1997) 227–239.

[42] G.B. Rouse, P.J. Miller, W.M. Risen, Mixed alkali glass spectra and structure, J. Non-Cryst. Solids 28 (1978) 193–207.

[43] S.K. Lee, G.D. Cody, B.O. Mysen, Structure and the extent of disorder in quaternary (Ca–Mg and Ca–Na) aluminosilicate glasses and melts, Am. Mineral. 90 (2005) 1393–1401.

[44] R.J. Kirkpatrick, R.K. Brow, Nuclear-magnetic-resonance investigation of the structures of phosphate and phosphate-containing glasses — a review, Solid State Nucl. Magn. Reson. 5 (1995) 9–21.

[45] R.K. Brow, C.C. Phifer, G.L. Turner, R.J. Kirkpatrick, Cation effects on P-31 Mas Nmr chemical-shifts of metaphosphate glasses, J. Am. Ceram. Soc. 74 (1991) 1287–1290.

[46] G.L. Turner, K.A. Smith, R.J. Kirkpatrick, E. Oldfield, Structure and cation effects on P-31 Nmr chemical-shifts and chemical-shift anisotropies of ortho-phosphates, J. Magn. Reson. 70 (1986) 408–415.

[47] R.K. Brow, R.J. Kirkpatrick, G.L. Turner, The short range structure of sodium-phosphate glasses.1. MAS NMR-studies, J. Non-Cryst. Solids 116 (1990) 39–45.

[48] J.M. Burnell, C. Liu, A.G. Miller, E. Teubner, Effects of dietary alteration of bicarbonate and magnesium on rat bone, Am. J. Physiol. 250 (1986) F302–F307.

[49] S. Bernick, G.F. Hungerford, Effect of dietary magnesium deficiency on bones and teeth of rats, J. Dent. Res. 44 (1965) 1317–1324.

[50] H.P. Dimai, S. Porta, G. Wirnsberger, M. Lindschinger, I. Pamperl, H. Dobnig, M. Wilders-Truschnig, K.H. Lau, Daily oral magnesium supplementation suppresses bone turnover in young adult males, J. Clin. Endocrinol. Metab. 83 (1998) 2742–2748.